J. Fluid Mech. (1981), *vol.* 110, *pp.* 335–347
Printed in Great Britain

Wave propagation over a rectangular trench

By JIIN-JEN LEE AND ROBERT M. AYER

Department of Civil Engineering, University of Southern California,
Los Angeles, California 90007

(Received 19 October 1979 and in revised form 30 December 1980)

An analysis is presented for the propagation of water waves past a rectangular submarine trench. Two-dimensional, linearized potential flow is assumed. The fluid domain is divided into two regions along the mouth of the trench. Solutions in each region are expressed in terms of the unknown normal derivative of the potential function along this common boundary with the final solution obtained by matching. Reflection and transmission coefficients are found for various submarine geometries. The result shows that, for a particular flow configuration, there exists an infinite number of discrete wave frequencies at which waves are completely transmitted. The validity of the solution in the infinite constant-water-depth region is shown by comparing with the results using the boundary integral method for given velocity distributions along the mouth of the trench. The accuracy of the matching procedure is also demonstrated through the results of the boundary integral technique. In addition, laboratory experiments were performed and are compared with the theory for two of the cases considered.

1. Introduction

A class of problems involving the propagation of water waves in a fluid of variable depth is one in which the depth is constant except for variations over a finite interval. Interest in these problems is largely due to the phenomena associated with the passage of waves over submarine trenches in the ocean and wave propagation across navigational channels, where changes in water depth are commonly the case. A general analysis of wave propagation over variable-depth geometries is given by Kreisel (1949). Kreisel's approach involves mapping the domain of the fluid into a rectangular strip, whereby the problem of solving for the velocity potential is reduced to a linear integral equation which can be solved by iteration for suitable geometries. A common method employed in the solution of problems involving changes in water depth is that of matching the solution along a geometrical boundary that separates the regions of different depths. Such an approach is found in the work of Bartholomeusz (1958) and Miles (1967). It has also been found by Newman (1965 *a*, *b*) and Black, Mei & Bray (1971) that for wave propagation over submarine obstacles there exists an infinite set of wavelengths such that the incident wave is totally transmitted.

Lassiter (1972) solved for the transmission and reflection coefficients in the case of monochromatic plane progressive surface waves over a rectangular submarine trench where the water depths before and after the trench are constant but not necessarily equal. Lassiter formulated the problem in terms of complementary variational integrals and solved for the velocity potential by matching the solution along vertical lines before and after the trench.

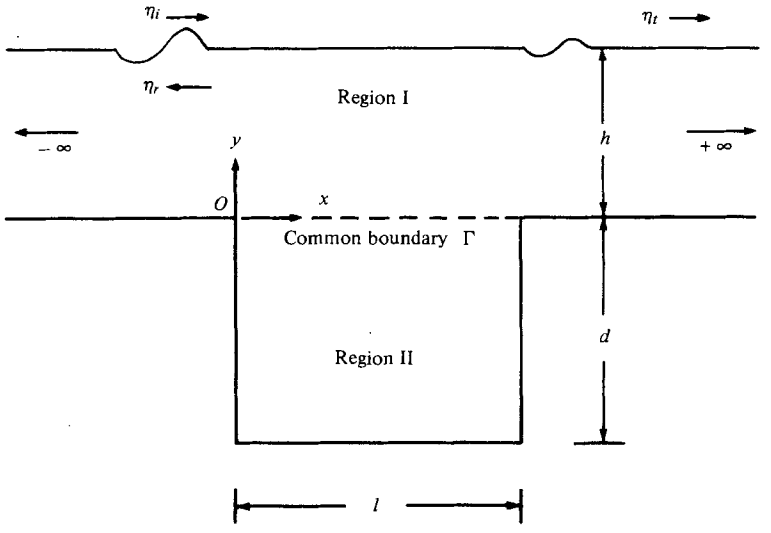

FIGURE 1. Definition sketch of the trench with regions of consideration.

In this present study, the problem considered is two-dimensional motion of linear periodic water waves over a rectangular submarine trench where the water depths before and after the trench are equal and constant. By drawing a horizontal line, the authors have separated the domain into two subregions, namely an infinite rectangular region of constant depth and a finite rectangular region representing the trench itself.

An analytic solution for each region is then found explicitly in terms of an unknown velocity distribution along the trench/constant-depth boundary. By superimposing a linear periodic incident wave of specified frequency in the infinite constant depth region, the final solution is obtained by matching the solutions in each subregion along the common boundary.

2. The boundary-value problem

Let (x, y) be a Cartesian co-ordinate system with $y = 0$ coinciding with the impermeable boundary of the constant-depth region as shown in the definition sketch in figure 1. Assuming a steady-state solution for the velocity potential in the form

$$\Phi(x, y; t) = \phi(x, y) e^{-i\sigma t}, \tag{1}$$

the potential function $\phi(x, y)$ must satisfy Laplace's equation throughout the fluid domain and the following boundary conditions:

$$\left.\begin{aligned} &\frac{\partial \phi}{\partial y} = \frac{\sigma^2}{g}\phi \quad \text{on} \quad y = h \quad \text{and} \quad -\infty < x < \infty; \\ &\frac{\partial \phi}{\partial y} = 0 \quad \text{on} \quad y = 0 \quad \text{and} \quad x < 0, \quad y = 0 \quad \text{and} \quad x > l, \\ &\qquad\qquad\qquad\qquad\qquad\qquad\qquad\qquad y = -d \quad \text{and} \quad 0 < x < l; \\ &\frac{\partial \phi}{\partial x} = 0 \quad \text{on} \quad x = 0 \quad \text{and} \quad -d \leqslant y \leqslant 0, \quad x = l \quad \text{and} \quad -d \leqslant y \leqslant 0. \end{aligned}\right\} \tag{2}$$

In (1), σ represents the circular frequency, 2π/wave period; $i = \sqrt{-1}$.

In order to solve for $\phi(x, y)$ in an efficient manner, the fluid domain is divided into two regions, I and II (as shown in figure 1), by the common boundary Γ which is defined by

$$y = 0, \quad 0 \leqslant x \leqslant l.$$

The strategy used herein is to solve for $\phi(x, y)$ in each respective region in terms of the unknown $\partial\phi/\partial y$ along the common boundary Γ. Thus, by matching the solutions in each region at Γ, one is able to obtain the final solution.

3. Region I solution

The scattered velocity potential in region I, ϕ_{I}, satisfies the same homogeneous boundary conditions as ϕ and the following additional conditions:

$$\frac{\partial\phi_{\mathrm{I}}}{\partial y} = q(x) \quad \text{on} \quad y = 0, \quad 0 < x < l; \tag{3}$$

$$\frac{\partial\phi_{\mathrm{I}}}{\partial x} = \pm ik\phi_{\mathrm{I}} \quad \text{on} \quad x \to \pm\infty, \quad 0 \leqslant y \leqslant h; \tag{4}$$

where $q(x)$ represents the unknown velocity distribution along the trench/constant-depth boundary, and k is the outgoing wavenumber at infinity.

The solution for ϕ_{I} is determined using the Fourier transform as

$$\phi_{\mathrm{I}}(x, y) = \frac{1}{2\pi}\int_{-\infty}^{\infty} \frac{\tilde{q}(k)}{k}\left[\frac{(k+\sigma^2/g)\,e^{k(y-h)} + (k-\sigma^2/g)\,e^{k(h-y)}}{(k+\sigma^2/g)\,e^{-kh} - (k-\sigma^2/g)\,e^{kh}}\right] e^{ikx}\,dk, \tag{5}$$

where $\tilde{q}(k)$ is the transform of the still unknown function $q(x)$ represented approximately by

$$q(x) \cong \sum_{j=1}^{N} Q_j[H(x-x_{j-1}) - H(x-x_j)], \tag{6}$$

where the interval $0 < x < l$ has been partitioned into N segments of equal length, Q_j is the average value of $q(x)$ in the jth subinterval ($j = 1, 2, \ldots, N$), and $H(x-\xi)$ is the Heaviside step function.

A Fourier transform of (6) and substitution into (5) yields

$$\phi_{\mathrm{I}}(x,y) = \frac{1}{2\pi i}\sum_{j=1}^{N} Q_j[I_{j-1} - I_j],$$

where

$$I_j = \int_{-\infty}^{\infty} \frac{e^{ik(x-x_j)}}{k^2}\left[\frac{(k+\sigma^2/g)\,e^{k(y-h)} + (k-\sigma^2/g)\,e^{k(h-y)}}{(k+\sigma^2/g)\,e^{-kh} - (k-\sigma^2/g)\,e^{kh}}\right] dk.$$

To compute the integral defined by I_j, contour integration has been used; the integral I_j has simple poles at 0, $\pm k_r$ and $\pm ik_n$ ($n = 1, 2, \ldots$), where k_r and k_n are defined by the following relationships:

$$\frac{\sigma^2}{q} = k_r \tanh(k_r h) \quad \text{and} \quad \frac{\sigma^2}{g} = -k_n \tan(k_n h).$$

In order to obtain an outgoing wave solution (4) from the trench, we specify our inversion path to lie above the pole at $-k_r$ and below the pole at $+k_r$. For such a path, the solution for ϕ_{I} can be described as follows:

(1) If $x > x_j$ for all j,

$$\phi_{\mathrm{I}}(x,y) = \sum_{j=1}^{N} Q_j \left\{ \frac{[\exp[ik_r(x-x_j)] - \exp[ik_r(x-x_{j-1})]]}{k_r^2} S_r(k_r,y) + \sum_{n=1}^{\infty} \frac{[\exp[-k_n(x-x_{j-1})] - \exp[-k_n(x-x_j)]]}{k_n^2} S_n(k_n,y) \right\}. \tag{7}$$

(2) If $x < x_j$ for all j,

$$\phi_{\mathrm{I}}(x,y) = \sum_{j=1}^{N} Q_j \left\{ \frac{[\exp[-ik_r(x-x_{j-1})] - \exp[-ik_r(x-x_j)]]}{k_r^2} S_r(k_r,y) + \sum_{n=1}^{\infty} \frac{[\exp[k_n(x-x_j)] - \exp[k_n(x-x_{j-1})]]}{k_n^2} S_n(k_n,y) \right\}. \tag{8}$$

(3) If $x > x_{\mathrm{j}-1}$ and $x < x_{\mathrm{j}}$ for some $\mathbf{j}$,

$$\begin{aligned}\phi_{\mathrm{I}}(x,y) = {} & \sum_{j=1}^{\mathrm{j}-1} Q_j \left\{ \frac{[\exp[ik_r(x-x_j)] - \exp[ik_r(x-x_{j-1})]]}{k_r^2} S_r(k_r,y) + \sum_{n=1}^{\infty} \frac{[\exp[-k_n(x-x_{j-1})] - \exp[-k_n(x-x_j)]]}{k_n^2} S_n(k_n,y) \right\} \\ & + Q_{\mathrm{j}} \left[\frac{1+(\sigma^2/g)(y-h)}{\sigma^2/g} - \frac{[\exp[ik_r(x-x_{\mathrm{j}-1}) + \exp[-ik_r(x-x_{\mathrm{j}})]]}{k_r^2} S_r(k_r,y) + \sum_{n=1}^{\infty} \frac{[\exp[-k_n(x-x_{\mathrm{j}-1})] + \exp[k_n(x-x_{\mathrm{j}})]]}{k_n^2} S_n(k_n,y) \right] \\ & + \sum_{\mathrm{j}+1}^{N} Q_j \left\{ \frac{[\exp[-ik_r(x-x_{j-1})] - \exp[-ik_r(x-x_j)]]}{k_r^2} S_r(k_r,y) + \sum_{n=1}^{\infty} \frac{[\exp[k_n(x-x_j)] - \exp[k_n(x-x_{j-1})]]}{k_n^2} S_n(k_n,y) \right\}. \end{aligned} \tag{9}$$

In (7)–(9) the functions S_r and S_n are defined by

$$S_r(k_r,y) = \frac{k_r \cosh[k_r(y-h)] + (\sigma^2/g)\sinh[k_r(y-h)]}{k_r h \operatorname{sech} k_r h + \sinh k_r h},$$

and

$$S_n(k_n,y) = \frac{k_n \cos[k_n(y-h)] + (\sigma^2/g)\sin[k_n(y-h)]}{k_n h \sec k_n h + \sin k_n h}.$$

4. Region II solution

Again, the solution ϕ_{II} in region II satisfies the no-flow condition at the solid boundaries and the following condition:

$$\frac{\partial \phi_{\mathrm{II}}}{\partial y} = q(x) \quad \text{on} \quad y = 0, \quad 0 \leqslant x \leqslant l. \tag{10}$$

There exists a constraint on $q(x)$ (due to the conservation of mass in region II):

$$\sum_{j=1}^{N} Q_j = 0. \tag{11}$$

This condition must be also applied to region I.

Via the technique of separation of variables, the solution for the potential ϕ_{II} subject to the boundary conditions (2) and (10) is

$$\phi_{II}(x,y) = \alpha_0 + \sum_{n=1}^{\infty} \alpha_n \cos\frac{n\pi x}{l} \cosh\frac{n\pi(y+d)}{l}, \tag{12}$$

where α_0 is a constant which is determined by the matching procedure described in the next section, and α_n $(n \geqslant 1)$ is given by

$$\alpha_n = \frac{2}{n\pi \sinh(n\pi d/l)} \int_0^l q(x) \cdot \cos(n\pi x/l)\, dx. \tag{13}$$

5. Superposition and matching of solutions

For a periodic incident wave travelling in the positive x direction in region I, the velocity potential can be specified as

$$\Phi_{in}(x,y;t) = \phi_{in}(x,y)\, e^{-i\sigma t} = \frac{agi}{\sigma} \frac{\cosh k_r y}{\cosh k_r h} \exp[i(k_r x - \sigma t)]. \tag{14}$$

Defining $\hat{x}_j (j = 1, 2, \ldots, N)$ as the midpoint of the jth subinterval of Γ, we may in turn define the vectors $\{\phi_{in}\}$ and $\{\phi_I\}$ by

$$\phi_{in}^{(j)} = \phi_{in}(\hat{x}_j, 0) = \frac{agi}{\sigma} \operatorname{sech} k_r h \exp[ik_r \hat{x}_j] \quad (j = 1, 2, \ldots, N), \tag{15}$$

and

$$\phi_I^{(j)} = \phi_I(\hat{x}_j, 0) \quad (j = 1, 2, \ldots, N). \tag{16}$$

Using (9), it can be seen that $\{\phi_I\} = [H]\{Q\}$, where H is symmetric and

$$Q^{(j)} = Q_j \quad (j = 1, 2, \ldots, N).$$

Defining the column vector $\{\phi_{II}\}$ by $\phi_{II}^{(j)} = \phi_{II}(\hat{x}_j, 0)$, (6), (12), and (13) give

$$\{\phi_{II}\} = \{\beta_0\} + [S]\{Q\}, \tag{17}$$

where $\{\beta_0\}_{N\times 1}$ is a vector in which each member is (the same) arbitrary constant and $[S]$ is a real and symmetric $N \times N$ matrix.

Owing to the continuity of velocity potential along the common boundary Γ we have

$$\{\phi_{in}\} + \{\phi_I\} = \{\phi_{II}\}. \tag{18}$$

Substituting (15)–(17) into (18) we obtain N equations with $N+1$ unknowns (Q_1, $Q_2, \ldots, Q_N$ and β_0). However, (11) must again be implemented for region I, providing us with an additional equation. This system of linear equations is then solved numerically for the vector $\{Q\}$. Thus, the originally unknown function $q(x)$ introduced in (3) is now solved as a discrete vector $\{Q\}$.

N,P	K_t $(h/\lambda = 0{\cdot}05)$	K_t $(h/\lambda = 0{\cdot}10)$	K_t $(h/\lambda = 0{\cdot}15)$	K_t $(h/\lambda = 0{\cdot}20)$
5,5	0·7669	0·9471	0·9678	0·9982
10,10	0·7712	0·9717	0·9928	1·0000
15,15	0·7719	0·9761	0·9953	0·9999
30,30	0·7724	0·9793	0·9967	0·9997
50,50	0·7725	0·9802	0·9971	0·9997

TABLE 1. Values of K_t computed for different values of N, P and h/λ $(h = 4'', d = 26\frac{1}{2}'', l = 42\frac{3}{8}'')$.

6. Analysis of wave amplitude

Since the values Q_j have been found, the velocity potential in the entire domain is completely solved. In particular, the values of ϕ_{I} and ϕ_{in} at the surface can now be computed using (7)–(9) and (14). The wave amplitude at the water surface is given by linear theory to be

$$\eta = \frac{1}{g}\left|\frac{\partial \Phi_{\mathrm{I}}}{\partial t} + \frac{\partial \Phi_{\mathrm{in}}}{\partial t}\right|_{y=h} = \frac{\sigma}{g}\left|\phi_{\mathrm{I}} + \phi_{\mathrm{in}}\right|_{y=h},$$

at any value of x.

All of the theoretical results presented in figures 3–7 are computed when the trench length is divided into $N = 30$ equal segments and $P = 30$ terms are taken in the Fourier series (12).

In table 1, the accuracy of the computation of the transmission coefficient K_t is shown for various values of N and P at different values of h/λ for the case $h = 4''$, $d = 26\frac{1}{2}''$, $l = 42\frac{3}{8}''$.

It can be seen from the above table that $N = P = 30$ is of sufficient accuracy for a wide range of h/λ for this particular geometric configuration, and similar results were found for all of the cases presented.

The solution for the scattered wave potential ϕ_{I} given by (7)–(9) has also been verified independently by the boundary integral method, which is discussed by Lee (1971) and has been applied successfully in solving Laplace's equation for the velocity potential in two dimensions by Raichlen & Lee (1978).

Considering region I only, suppose that a vertical displacement $\xi(x)\, e^{-i\sigma t}$ is specified on $y = 0$, $0 < x < l$. Then the derivative is

$$q(x) = -i\sigma\xi(x), \quad 0 < x < l.$$

Using (7)–(9), the wave amplitude η can be computed at any value of x due to the bottom displacement $\xi(x)\, e^{-i\sigma t}$.

With respect to the boundary integral method, a finite region of sufficient length from the disturbance must be taken to accurately represent the boundary conditions at infinity and a sufficiently large number of boundary elements must be chosen.

In table 2 a comparison is made of the quantity η_∞/ξ_0 between the region I solution given by (7) and that obtained by the boundary integral method at various values of h/λ_∞; η_∞ is the wave amplitude at $x \to +\infty$, ξ_0 is the maximum of $\xi(x)$ on $0 < x < l$, and λ_∞ is the length of the outgoing wave at infinity. In this table, $N = 30$ segments covering the boundary of the trench mouth are used in the region I solution. A distance

$\frac{h}{\lambda_\infty}$	$\frac{\eta_\infty}{\xi_0}$ (present method)	$\frac{\eta_\infty}{\xi_0}$ (B.I.M.)
0·05	0·396	0·380
0·10	0·689	0·693
0·15	0·809	0·797
0·20	0·744	0·740

TABLE 2. Comparison of the value of η_∞/ξ_0 between the boundary integral method and present method ($\xi_0/h = 0{\cdot}1$, $\xi(x) = \xi_0$, $h = 8''$, $l = 21\frac{1}{8}''$).

of 3·0 feet was taken from the bottom disturbance and 120 boundary elements were employed in the entire boundary treated by boundary integral method.

Table 2 shows a comparison of η_∞/ξ_0 for $\xi_0/h = 0{\cdot}1$ at various values of h/λ_∞ for the configuration $h = 8''$, $l = 21\frac{1}{8}''$. The displacement $\xi(x)$ is given by a uniform displacement $\xi(x) = \xi_0$ which is representative of a piston-like bottom motion on $0 < x < l$.

The fact that the results from the boundary integral method become less accurate for extreme values of h/λ_∞, should be taken into account. In the case of shallow water waves, the finite region employed becomes too small compared with the wavelength, and for high-frequency waves the velocity potential varies too much between boundary elements for accurate computation, if the total number of boundary elements remains the same. Nevertheless, the comparison shown in table 2 verifies the solution given by (7). Further, the accuracy of the matching procedure was verified by using the boundary integral method to solve for the solution in region II in lieu of (12) & (13). Seventy-five boundary elements were distributed along the boundary of region II and the solution in terms of Q_j ($j = 1, 2, \ldots, N$) was matched with the region I solution as per the matching equation (18). The result plotted in figure 6 shows excellent agreement with the result of the present method.

7. Experimental equipment and procedure

A series of laboratory experiments has been conducted in a wave tank 12 inches wide, 48 feet long and 18 inches deep. A paddle-type wave generator is placed at one end of the tank to generate the desired wave at a specified wave period. The wave period is controlled by a variable-speed motor control. A wave filter is placed in front of the wave paddle while a wave absorber is located at the end of the wave tank. At the central section of the wave tank a special trench section is installed. The trench section extends $26\frac{1}{2}''$ below the bottom of the wave tank to rest on the laboratory floor. The maximum trench length is 85 inches. Four different trench lengths can be obtained through the partitions installed, namely $21\frac{1}{8}''$, $42\frac{3}{8}''$, $63\frac{5}{8}''$, $85''$. The depth in the trench section can also be varied by placing a false bottom at various heights.

The wave amplitude is measured by means of resistant-type wave gauges. The wave records are recorded using a Hewlett Packard four-channel oscillograph.

Wave amplitudes were measured in the region 2 feet to 6 feet behind the trench section. Wave-amplitude envelopes are obtained first without the effect of the trench (by covering the trench section completely) in order to determine the incident wave amplitude. The wave envelopes are then obtained with the trench at the desired length

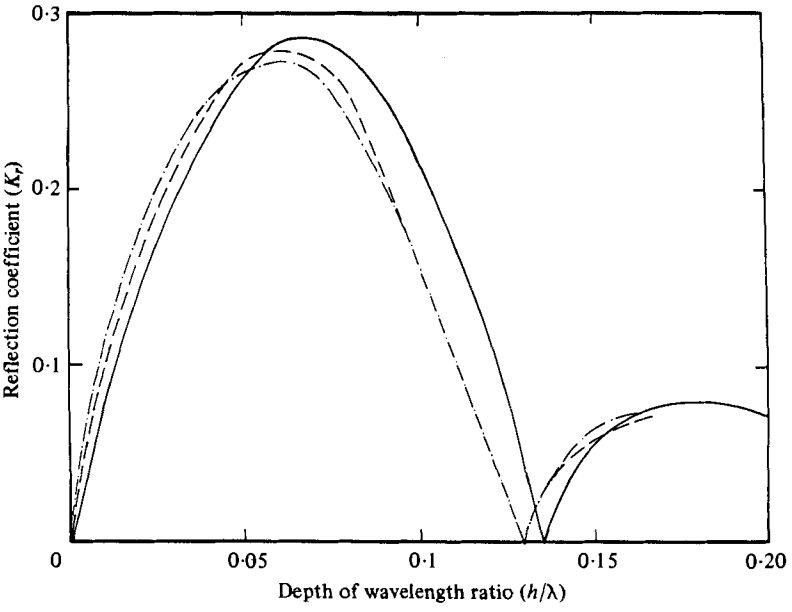

FIGURE 2. Comparison of reflection coefficient with results of Lassiter (1972) ($h = 4''$, $d = 4''$, $l = 20''$). ——, present results; — — — —, —·—·—·—, Lassiter's results.

and depth at the same region behind the trench section in order to ascertain the wave amplitude after passing over the trench section. The wave envelopes at the region between the wave generator and the location of the trench are not measured.

8. Presentation and discussion of results

The effect of the trench on the propagation of waves can be demonstrated most easily by the transmission and reflection characteristics. In all figures, the transmission and reflection coefficients, K_t and K_r, are shown as functions of the relative wavelength. The ordinate is the ratio of the transmitted wave amplitude divided by the incident wave amplitude, while the abscissa is the ratio of the water depth (h) in region I divided by the incident wavelength (λ). The wavelength λ is computed from the dispersion relationship, $\lambda = (gT^2/2\pi)\tanh(2\pi h/\lambda)$, where T is the incident wave period.

A comparison of the reflection coefficient obtained by the present method along with the work of Lassiter (1972) is shown in figure 2. As can be seen, the results of the proposed method compare well with those obtained by the variational approach employed by Lassiter. It is also shown by Lassiter that the two curves he obtained represent upper and lower bound solutions to the variational method used. Such a definite conclusion concerning upper and lower bounds cannot be reached by the present method. However, the present solution scheme provides an explicit analytic solution as given in (7) to (9) once the values of Q_j are obtained by matching.

Figures 3–7 show the effect on the wave transmission and reflection as a function of trench length, trench depth and water depth. From figure 3 the incident waves are almost fully transmitted for $h/\lambda > 0{\cdot}18$. At $h/\lambda = 0{\cdot}09$, the transmission coefficient reaches a minimum at approximately 0·89. The corresponding values of l/λ for h/λ

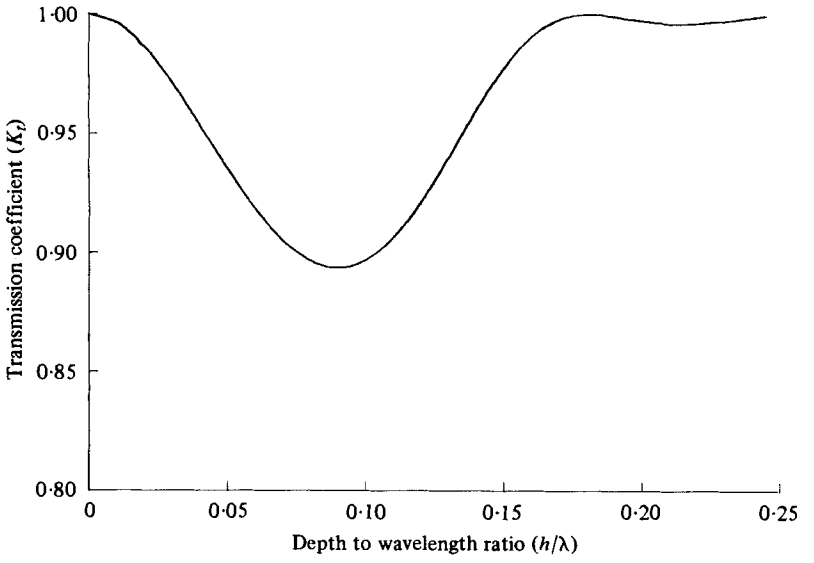

FIGURE 3. Transmission coefficient as a function of relative wavelength ($h = 4''$, $d = 26\frac{1}{2}''$, $l = 21\frac{1}{8}''$).

$= 0{\cdot}18, 0{\cdot}09$ are: 0·95 and 0·475. It appears that for a relatively short trench length, in a rather deep trench, the maximum reduction of transmitted wave occurs as l/λ approaches 0·5. As the wave period is decreased to where l/λ approaches 1, the effect on wave transmission due to the trench is negligible. This can be explained in the following:

For such a relatively short trench length, as l/λ approaches 1, the vertical velocity of water particles at the trench mouth nearly satisfies the requirement of (11), i.e. the conservation of mass condition for region II. Therefore, the minimum effect is experienced by the propagating waves and the transmission coefficient is almost equal to 1. For the case of l/λ approaching 0·5 the incident wave must undergo a drastic adjustment in order to satisfy (11). Therefore, the transmission coefficient is reduced to a minimum for this particular wave frequency.

Although this explanation may be considered helpful it cannot explain the location of each peak and trough in the curves of transmission coefficient presented in this paper. One reason is that the effect of the trench is rather complicated as regions I and II are dynamically interacting. Also, the value of the wavelength λ is based on the water depth in region I (h). Hence the true wavelength at the trench region differs from λ, so that the propagating wave does not instantly adjust to the new depth as it passes over the trench. As a result, one is not certain which λ should be used in order to adequately explain the effect of the trench.

Figure 4 shows the computed reflection coefficient as a function of the relative wavelength for the same range of h/λ shown in figure 3. The reflection coefficient, K_r, is defined as the reflected wave amplitude divided by incident wave amplitude. As expected, the maximum reflected wave occurs at $h/\lambda = 0{\cdot}09$ where the transmitted wave is a minimum. As this is an inviscid theory, one can check the result to see whether $K_r^2 + K_t^2 = 1$ can be satisfied (where K_r is the reflection coefficient, K_t the transmission coefficient). For the range of h/λ, it is checked that such a relation holds true; thereby further increasing the validity of the theoretical result.

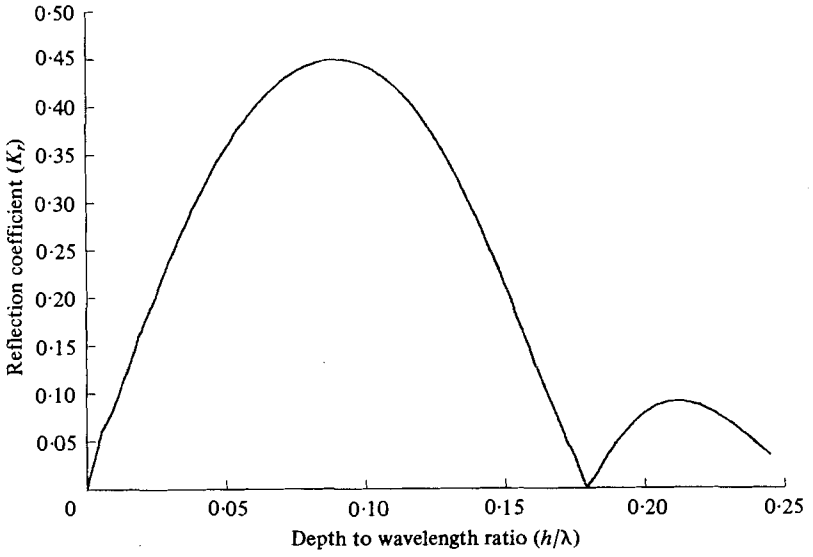

FIGURE 4. Reflection coefficient as a function of relative wavelength ($h = 4''$, $d = 26\frac{1}{2}''$, $l = 21\frac{1}{8}''$).

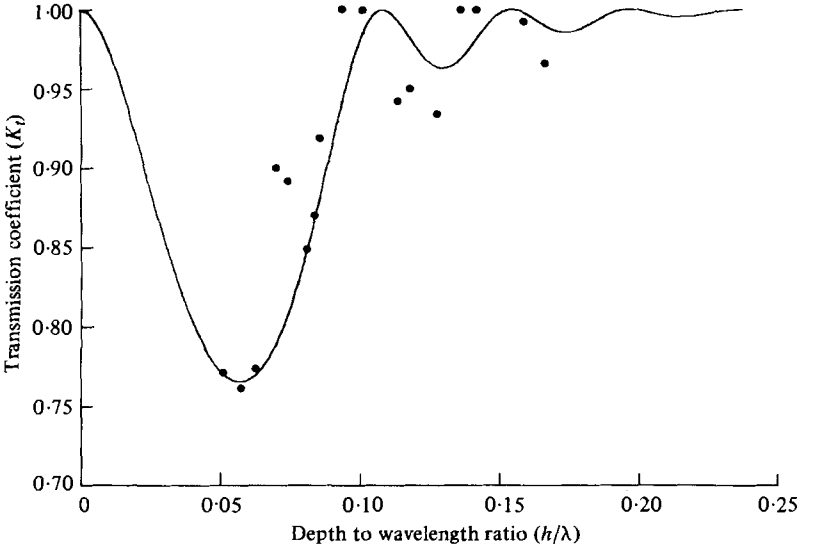

FIGURE 5. Transmission coefficient as a function of relative wavelength ($h = 4''$, $d = 26\frac{1}{2}''$, $l = 42\frac{3}{8}''$). ——, theoretical results; ●, experimental results.

As the trench length increases, the effect of the trench on transmission and reflection characteristics becomes more interesting. This is shown in figure 5. The trench length for this case is twice the length of that in figures 3 and 4. It is seen for the range of h/λ presented, there are four wave periods at which waves are fully transmitted ($K_t = 1$, $K_r = 0$). The reduction in transmission coefficient or increase in reflection coefficient is more pronounced at $h/\lambda = 0{\cdot}056$. Again, it is seen that the effect of the trench on transmission or reflection coefficients for higher values of h/λ is decreasingly smaller.

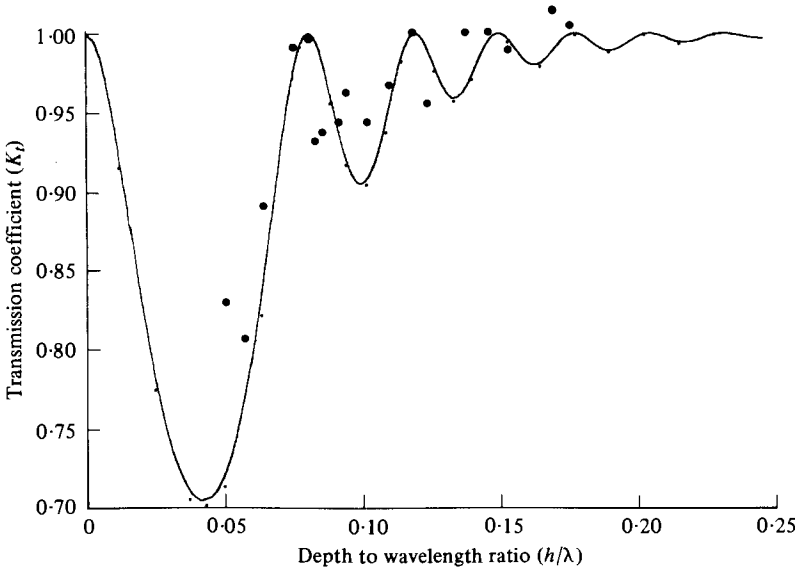

FIGURE 6. Transmission coefficient as a function of relative wavelength ($h = 4''$, $d = 26\frac{1}{2}''$, $l = 63\frac{5}{8}''$). ——, present theoretical results; ●, experimental results; ., results using boundary integral method.

This is reasonable because, for higher values of h/λ, the water depth is relatively deeper.

In figure 5 experimental data on the transmission coefficient has been included for comparison. It is seen that the experimental data in general confirms the trend predicted by the theoretical analysis. Also apparent from the experimental data is that there exists an oscillation of data points about the theoretical curve. This could be due to the effect of the finite length of the wave tank and that the wave absorbers placed at both ends of the wave tank cannot eliminate the wave reflection completely from the tank ends.

Results on wave transmission over a longer trench length is shown in figure 6. The trench length for this case is three times that shown in figure 3 with other dimensions held constant. In the range of $0 < h/\lambda < 0{\cdot}25$, there are six different wave periods at which waves are fully transmitted. The results indicate that the trench does exert a greater influence on wave transmission on wave characteristics in that the transmission coefficient at $h/\lambda = 0{\cdot}042$ is only about 0·70. Experimental data are also included in figure 6. It is seen that the experimental data in general tend to confirm the theoretical prediction. However, due to experimental errors and the unavoidable wave reflections from both ends of the wave tank, the experimental data show considerable scattering as evident in the figure. Results obtained by using boundary integral method for region II solution matching with the solution from region I is also included for comparison. It is seen that the two theoretical results agree very well.

To show the effect of the water depth in the trench, the depth of the trench in figure 7 is changed to $d = 13\frac{1}{4}$ inches (one-half of that presented in figure 6). As may be expected the values of h/λ corresponding to peaks and troughs in the response curve are slightly different. While there is an increase in the wave transmission for the first trough, the

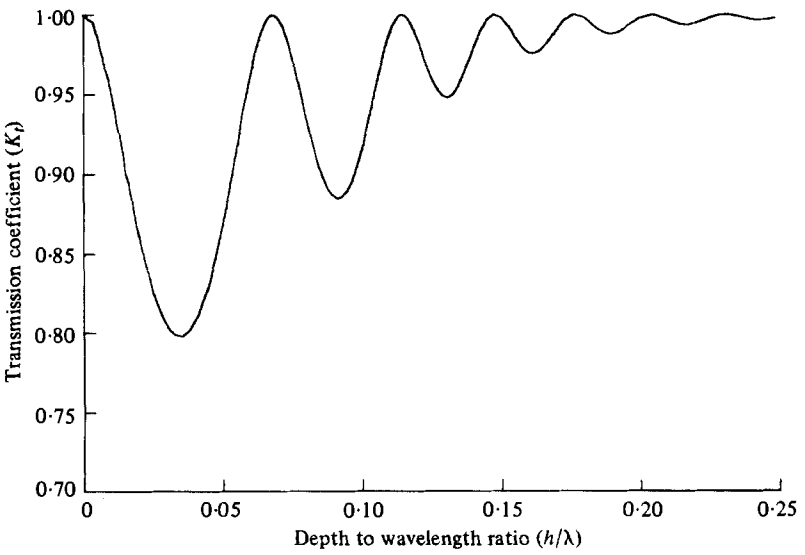

FIGURE 7. Transmission coefficient as a function of relative wavelength ($h = 4''$, $d = 13\frac{1}{4}''$, $l = 63\frac{3}{8}''$).

wave transmission for the second trough is somewhat decreased. This follows because a decrease in the value of d means that the trench would not be so deep as to fall in the deep-water wave range completely.

9. Concluding remarks

The analytic method outlined for analysing the effect of a rectangular trench on the propagation of periodic incident waves has been shown to be quite effective as illustrated by comparison with other solution techniques and with experiments. From the results on wave transmission and reflection, it is seen that there exists an infinite number of wave periods at which waves are fully transmitted. An attempt has been made to explain this phenomenon physically. The effect of the trench on wave transmission (or reflection) is progressively smaller for higher wave frequencies (the larger values of h/λ).

The work reported herein is supported by the National Science Foundation under Grant no. ENV77-01599 and by N.O.A.A. Sea Grant under Grant no. 04-80M01-186. The help of Mr Kamran Irajpanah and Mr C. M. Ma on the experimental work is greatly appreciated. The authors would like to thank Dr H. L. Wong for helpful discussions. The authors also wish to thank Professor J. N. Newman for providing Dr J. B. Lassiter's thesis for reference.

REFERENCES

BARTHOLOMEUSZ, E. F. 1958 The reflection of long waves at a step. *Proc. Camb. Phil. Soc.* **54**, 106–118.

BLACK, J. L., MEI, C. C. & BRAY, M. C. G. 1971 Radiation and scattering of water waves by rigid bodies. *J. Fluid Mech.* **46**, 151–164.

KREISEL, H. 1949 Surface waves. *Quart. Appl. Math.* **7**, 21–44.

LASSITER, J. B. 1972 The propagation of water waves over sediment pockets. Ph.D. thesis, Massachusetts Institute of Technology.

LEE, J. J. 1971 Wave induced oscillations in harbours of arbitrary geometry. *J. Fluid Mech.* **45**, 375–394.

MILES, J. W. 1967 Surface-wave scattering matrix for a shelf. *J. Fluid Mech.* **28**, 755–767.

NEWMAN, J. N. 1965 Propagation of water waves past long two-dimensional obstacles. *J. Fluid Mech.* **23**, 23–29.

NEWMAN, J. N. 1965 Propagation of water waves over an infinite step. *J. Fluid Mech.* **23**, 399–415.

RAICHLEN, F. & LEE, J. J. 1978 An inclined-plate wave generator. *Proc. 16th Int. Coastal Eng. Conf.* Hamburg, Germany, pp. 388–399.